

Diffraction by volume gratings with imaginary potentials

M V Berry and D H J O'Dell

H H Wills Physics Laboratory, Tyndall Avenue, Bristol BS8 1TL, UK

Received 13 November 1997

Abstract. A medium described by an imaginary potential (or imaginary (refractive index)²), that varies sinusoidally in one direction, acts as a volume grating for plane waves incident on it obliquely or normally. Two peculiar features are identified. First, if the potential is weak, so that there are only two significant diffracted beams near the Bragg angle, and three for normal incidence, diffraction is strongly affected by degeneracies of the non-Hermitian matrix generating the 'Bloch waves' in the grating; the effect of these degeneracies is very different from that of the Hermitian degeneracies for transparent gratings. Second, if the potential is strong and the grating thick, the asymptotic distribution of intensities among the diffracted beams (momentum distribution) is a rather narrow Gaussian, and dominated by a single set of complex rays; this is very different from the semiclassical limit for transparent gratings, where the rays form families of caustics proliferating with thickness, and with a wider momentum distribution.

1. Introduction

Our purpose here is to draw attention to several curious features of wave propagation in periodic structures ('gratings') where the potential is purely imaginary, in contrast to the more familiar potentials that are real (no dissipation) or have a small imaginary part (weak dissipation). In the simplest nontrivial problem of this sort, the purely dissipative potential varies sinusoidally in only one direction (x), and the wave ψ propagates paraxially in two dimensions (x, z). Such phenomena are governed by

$$\nabla^2 \psi(x, z) + (k^2 + iQ \cos^2(Kx)) \psi(x, z) = 0 \quad (1)$$

where $K \ll k$ and Q is real (the usual case of a transparent medium would have $Q = iQ_2$, where Q_2 is real).

We envisage (1) applying in a slab (volume grating) extending from $z = 0$ to $z = Z$. Because the operator in (1) is periodic, a plane wave incident from $z < 0$ will, notwithstanding the dissipation, emerge into the space $z > Z$ as a series of Bragg-diffracted beams. The amplitudes A_n of the beams obey the Raman–Nath equations (Raman and Nath 1936b) (section 2) that have been much studied in the transparent case of light diffracted by a grating of ultrasound (for a review, see Berry (1966)). But for imaginary gratings the non-Hermitian nature of the operator in (1) makes the behaviour of the intensities $P_n = |A_n|^2$ unusual in several respects.

First, they obey an unfamiliar sum rule (section 2). Second, the matrix governing the 'Bloch waves' inside the grating can be made degenerate by varying parameters (section 3). Now, degeneracies of non-Hermitian matrices are very different from degeneracies of Hermitian matrices, and the mathematical differences are reflected in the behaviour of the P_n (for other physical phenomena depending on degeneracies of non-Hermitian matrices,

see section 3 of Berry (1994)); these are particularly striking when Q is small, so the number of diffracted beams is small. Third, the opposite extreme, when Q is large (section 4) and the number of beams is large, is the imaginary counterpart of the semiclassical or geometrical-optics regime. However, the P_n are not dominated, as in the transparent case, by caustics (Lucas and Biquard 1932, Nomoto 1951) (singularities of families of rays) that proliferate and get more complicated as z increases, but by one simple set of rays that is surprisingly easy to calculate.

One situation where (1) occurs is in atom optics (Oberthaler *et al* 1996). A beam of atoms with three effective internal states, mass m and energy $E = \hbar^2 k^2 / 2m$ propagates through a standing-wave field with wavenumber K , produced, for example, by two counter-propagating laser beams. The three levels are a ground state and an excited state—these are the working levels—and a level to which the excited state decays. According to Chudesnikov and Yakovlev (1991), the quantum wave ψ for the centre of mass of the atoms remaining in the ground state is determined by the potential

$$V(x) = \frac{d^2 E_0^2}{\hbar (\Delta + \frac{1}{2}i\gamma)} \cos^2(Kx) \quad (2)$$

where Δ is the detuning of the laser beam from the transition frequency of the working levels, d the dipole matrix element for this transition, γ the decay rate from the excited to the third state, and E_0 is the electric field strength of the laser. The Hamiltonian involving this potential is non-Hermitian because ψ ignores those atoms decaying into the third level. It follows that the potential is purely imaginary if the detuning is zero, with Q in (1) given by

$$Q = \frac{4md^2 E_0^2}{\gamma \hbar^3}. \quad (3)$$

Another way to implement (1) is with the propagation of electromagnetic waves of frequency ω in a periodic medium with uniform (real) dielectric constant ε and (real) conductivity Σ varying sinusoidally with x , that is

$$\Sigma(x) = \Sigma_0 \cos^2(Kx). \quad (4)$$

Then it follows from Maxwell's equations that waves linearly polarized along y satisfy (1), with ψ representing the electric field component and

$$k^2 = \omega^2 \varepsilon \mu_0 \quad Q = \mu_0 \omega \Sigma. \quad (5)$$

The requirements that ε and Σ are real will be satisfied if these quantities represent the dc response of the material, with ω much smaller than all natural frequencies (e.g. in diffraction of microwaves by a stack of different metal plates).

2. Raman–Nath equations and intensity sum rule for diffracted beams

Let the wave incident from $z < 0$ be travelling at an angle $\theta = K_0/k \ll 1$ to the z axis, that is

$$\psi_{\text{inc}} = \exp\{i(k_0 z + K_0 x)\} \quad (6)$$

where $k^2 = k_0^2 + K_0^2$. In the medium, the corresponding solution of (1) can be written

$$\psi = \exp\{i(k_0 z + K_0 x)\} \sum_{n=-\infty}^{\infty} A_n(z) \exp(2inKx). \quad (7)$$

Emerging from the grating into the space $z > Z$ are the diffracted beams. $A_n(Z)$ is the amplitude of the n th beam, which travels in the direction $\theta + n\theta_B$, where $\theta_B = 2K/k$ is the Bragg angle.

Assuming paraxiality, that is $K \ll k$, the variation of the A_n with z will be much slower than $\exp(ikz)$. Then substitution of (7) into (1) gives, with the initial condition (6), the Raman–Nath equations for an imaginary grating:

$$\begin{aligned} \partial_\zeta A_n(\zeta) &= [-2in(n + \alpha) - \sigma] A_n(\zeta) - \frac{1}{2}\sigma [A_{n+1}(\zeta) + A_{n-1}(\zeta)] \\ A_n(0) &= \delta_{n,0} \end{aligned} \tag{8}$$

where

$$\zeta \equiv \frac{K^2 z}{k_0} \quad \alpha \equiv \frac{K_0}{K} = \frac{2\theta}{\theta_B} \quad \sigma \equiv \frac{Q}{4K^2}. \tag{9}$$

Because of the dissipation, we expect that the total intensity in all the beams (total energy) will not be conserved but should decay exponentially with increasing depth ζ . Surprisingly, this does not happen. The analogue of $\Sigma P_n = 1$ for the transparent case is easily found from (8) to be

$$\sum_{n=-\infty}^{\infty} (-1)^n P_n(\zeta) = \sum_{n=-\infty}^{\infty} (-1)^n |A_n(\zeta)|^2 = \exp(-2\sigma\zeta) \tag{10}$$

so that the exponentially decaying quantity is not the total energy but involves an alternating sum of the intensities. This sum rule provides a powerful check on numerical solutions of (8) (which are unstable), and has other consequences, as we will see.

3. Physics of non-Hermitian degeneracies: two and three beams

In this section we consider σ to be small. Then the coupling of the $n = 0$ (forward) beam with the others is small, except for incidence corresponding to the first Bragg reflection, namely $\alpha = -1$ (that is $\theta = -\theta_B/2$), in which case the $n = 1$ beam can be large too. To explore this two-beam case, we write

$$\alpha = -1 + \beta \tag{11}$$

so that β measures deviation from the Bragg angle, and include only A_0 and A_1 in the Raman–Nath equations (8). Thus

$$i\partial_\zeta \begin{pmatrix} A_0 \\ A_1 \end{pmatrix} = \mathbf{M} \begin{pmatrix} A_0 \\ A_1 \end{pmatrix} \quad \text{where} \quad \mathbf{M} = \begin{pmatrix} -i\sigma & -\frac{1}{2}i\sigma \\ -\frac{1}{2}i\sigma & 2\beta - i\sigma \end{pmatrix}. \tag{12}$$

In the transparent case, where $\sigma = i\sigma_2$, the matrix \mathbf{M} is Hermitian. For an imaginary potential, it is not. Its eigenvalues are

$$\lambda_\pm = \beta - i\sigma \pm \sqrt{\beta^2 - \frac{1}{4}\sigma^2} \tag{13}$$

and the eigenfunctions are

$$|\chi_\pm\rangle = \begin{pmatrix} -i\sigma \\ 2\left(\beta \pm \sqrt{\beta^2 - \frac{1}{4}\sigma^2}\right) \end{pmatrix}. \tag{14}$$

The diffracted amplitudes are obtained from the superposition of the eigenfunctions satisfying the initial condition in (8). This is

$$\left. \begin{aligned} \begin{pmatrix} A_0 \\ A_1 \end{pmatrix} &= B_+ |\chi_+\rangle \exp(-i\lambda_+\zeta) + B_- |\chi_-\rangle \exp(-i\lambda_-\zeta) \\ \text{where } B_{\pm} &= i \frac{\sqrt{\beta^2 - \frac{1}{4}\sigma^2 \mp \beta}}{2\sigma\sqrt{\beta^2 - \frac{1}{4}\sigma^2}} \end{aligned} \right\}. \quad (15)$$

We emphasize the degeneracy at $\beta = \pm\sigma/2$. This is a branch point for the eigenvalues and eigenfunctions: around a circuit in complex σ space, the $+$ and $-$ states exchange identities. As the degeneracy is approached, the two eigenvectors (14) become parallel, and the coefficients B_{\pm} diverge (of course the amplitudes themselves remain finite). This contrasts with the behaviour at degeneracies of Hermitian matrices: in the transparent case, where $\sigma = i\sigma_2$, the eigenvalues in β, σ_2 space form a double cone (diabolo) (Teller 1937) centred on the degeneracy at $\beta = \sigma_2 = 0$, around which the states $+$ and $-$ preserve their identities (each being confined to its own conical sheet) and remain orthogonal.

In the intensities corresponding to (15), the three variables ζ, β and σ can be replaced by two, that we define as

$$\eta \equiv \frac{1}{2}\zeta |\sigma| = \frac{z|Q|}{8k_0} \quad \delta \equiv \frac{2\beta}{|\sigma|} = \frac{4(\theta + \frac{1}{2}\theta_B)}{|\sigma|\theta_B}. \quad (16)$$

The degeneracy corresponds to $\delta = 1$. Then

$$\left. \begin{aligned} P_1 &\equiv |A_1|^2 = \exp(-4\eta) \frac{\sin^2(\eta\sqrt{\delta^2-1})}{\delta^2-1} \\ P_0 &\equiv |A_0|^2 = \exp(-4\eta) + P_1 \end{aligned} \right\}. \quad (17)$$

These formulas satisfy the alternating sum rule (10); they are valid for all η and δ if σ is small enough.

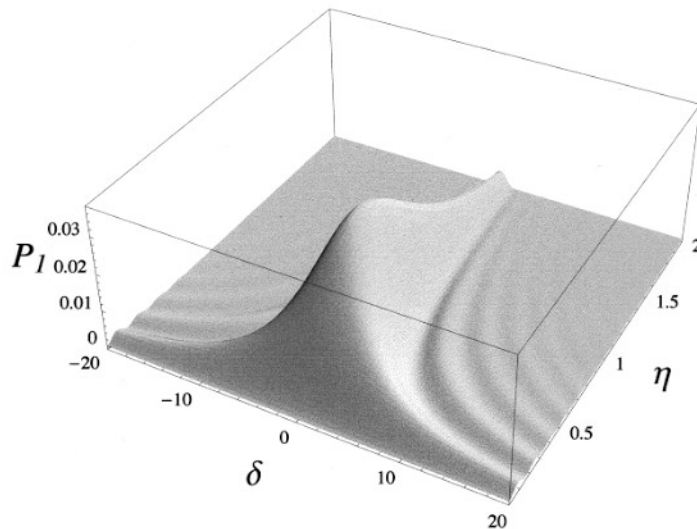


Figure 1. Intensity P_1 (equation (17)) of the first Bragg-reflected beam for an imaginary grating, as a function of the thickness and angular deviation variables η and δ defined by (16).

Figure 1 shows P_1 as a function of thickness η and deviation δ from the Bragg angle. The most notable feature is that the degeneracy $\delta = 1$ marks the transition from oscillatory

(trigonometric) to non-oscillatory (hyperbolic) behaviour of both the thickness dependence (variation with η for fixed δ) and the ‘rocking curves’ (variation with δ for fixed η), as demonstrated by the dark fringes of the pattern, at

$$\delta_n = \pm \sqrt{1 + \left(\frac{n\pi}{\eta}\right)^2} \quad (n = 1, 2, \dots) \quad (18)$$

whose asymptote as $\eta \rightarrow \infty$ is $\delta_n = 1$. Near the Bragg angle and for thick gratings, the decay of the rocking curve is Gaussian, namely

$$P_1 \approx \frac{1}{4} \exp(-2\eta) \exp(-\delta^2 \eta) \quad (\eta \gg 1, \delta \ll 1) \quad (19)$$

with the angular width of the Bragg peak shrinking with thickness as $\Delta\delta \sim 1/\sqrt{\eta}$. From (17), the same decay applies to the total intensity $P_0 + P_1$ of the transmitted atoms. Alternatively stated, the total transmitted intensity increases anomalously at the Bragg angle, a ‘remarkable phenomenon’ predicted and observed by Oberthaler *et al* (1996) and related to the effect discovered long ago by Borrmann (1941) for X-rays diffracted by an absorbing crystal.

By contrast, the intensities for a transparent grating, with $\sigma = i\sigma_2$ and the variables still defined by (16), are

$$\left. \begin{aligned} P_1 &= \frac{\sin^2(\eta\sqrt{\delta^2+1})}{\delta^2+1} \\ P_0 &= 1 - P_1 \end{aligned} \right\}. \quad (20)$$

Now the fringes in the η, δ plane cross the Bragg axis $\delta = 0$, and $\eta = n\pi$, and the total transmitted intensity is unity irrespective of the direction δ .

It is, however, possible to get degeneracies between Bloch waves for transparent gratings. In the many-beam transmission electron microscopy of thin crystals, where the crystal potential is not a single sinusoid but has many Fourier components, degeneracies can be produced at Bragg angles by varying the voltage of the microscope, and the ‘critical voltage effect’ (Buxton and Berry 1974, 1976, Berry *et al* 1973) can be detected by the divergence of the spacing of ‘bend contours’ (fringes of thickness and orientation).

Degeneracy can also occur for normal incidence ($\alpha = 0$) with σ small. Then all amplitudes are negligible except A_0 and $A_{+1} = A_{-1}$. The Raman–Nath equations for this three-beam case are

$$i\partial_\zeta \begin{pmatrix} A_0 \\ A_1 \end{pmatrix} = \mathbf{N} \begin{pmatrix} A_0 \\ A_1 \end{pmatrix} \quad \text{where} \quad \mathbf{N} = \begin{pmatrix} -i\sigma & -i\sigma \\ -\frac{1}{2}i\sigma & 2 - i\sigma \end{pmatrix}. \quad (21)$$

\mathbf{N} has eigenvalues

$$\lambda_\pm = 1 - i\sigma \pm \sqrt{1 - \frac{1}{2}\sigma^2}. \quad (22)$$

This time the degeneracy is at $\sigma = \sqrt{2}$. Solving (21) gives the intensities as

$$\left. \begin{aligned} P_{\pm 1} &\equiv |A_{\pm 1}|^2 = \exp(-2\sigma\zeta) \frac{\sigma^2}{4\left(1 - \frac{1}{2}\sigma^2\right)} \sin^2\left(\zeta\sqrt{1 - \frac{1}{2}\sigma^2}\right) \\ P_0 &\equiv |A_0|^2 = \exp(-2\sigma\zeta) + 2P_1 \end{aligned} \right\} \quad (23)$$

which satisfy the alternating sum rule (10). At the degeneracy,

$$P_{\pm 1} = \frac{1}{2}\zeta^2 \exp(-2^{3/2}\zeta) \quad P_0 = (1 + \zeta^2) \exp(-2^{3/2}\zeta) \quad (24)$$

and as before this marks the transition from oscillatory to hyperbolic behaviour. Figure 2 shows that $\sigma = \sqrt{2}$ is within the range of the three-beam approximation, at least in the region where the intensities are appreciable. For larger ζ , the exact solutions of the

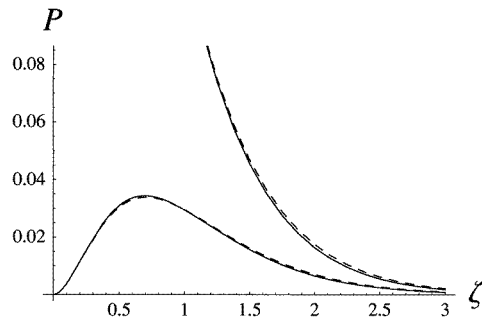


Figure 2. Dashed curves: intensities P_0 (upper curve) and P_1 (lower curve) at normal incidence, in the three-beam approximation (24) for the grating strength $\sigma = \sqrt{2}$, for which the governing matrix (21) is degenerate; full curves: scaled intensities from the full Raman–Nath equations (8) for $\alpha = 0$.

Raman–Nath equations (8) diverge from the approximations (24), because of contributions from the beams with $|n| \geq 2$ (even when these are small, they can vary rapidly as a result of the factor $2in^2$ in (8) with $\alpha = 0$, and so can spoil the three-beam approximation through their derivatives).

4. Nonclassical semiclassical behaviour: many beams

Now we consider large σ , that is gratings acting strongly on the waves passing through them. We restrict ourselves to normal incidence, that is $\alpha = 0$. The aim is to determine the asymptotic distribution of the intensities P_n as the grating thickness Z increases.

If the grating were transparent, that is $\sigma = i\sigma_2$, this would be the geometrical optics regime, and the solutions of the Raman–Nath equations could be obtained (Berry 1966) in terms of the rays bent by the sinusoidal refractive index in (1): the P_n would be given approximately by the transverse momentum distribution of the rays leaving the grating at $z = Z$ in the direction of the n th Bragg-diffracted beam. The non-negligible intensities would be those with $|n| < \sqrt{\sigma_2}$ (corresponding to the maximum slope of the rays), and the pattern of intensities would be dominated by *caustics* in the momentum distribution. As z increases, the caustics would get more numerous, and the corresponding asymptotics of the diffracted beams would get more complicated.

With the imaginary grating, the intensities behave very differently. It is still possible to think formally in terms of rays, but now these are complex, and for large z the only rays that survive are those traversing the grating near the minima of $\cos^2(Kx)$ in (1). These rays wind like particles in a harmonic potential well, and they are unaffected by the periodicity of the grating. It is possible to incorporate this insight into a geometrical optics theory for the complex rays, but it is complicated to implement. A more direct procedure that yields exactly the same results is to solve the Raman–Nath equations directly, regarding the index n as a continuous variable.

It is convenient first to rewrite (8) in the different variables B_n , defined by

$$A_n(\zeta) \equiv (-1)^n B_n(\zeta). \quad (25)$$

Thus (for normal incidence)

$$\begin{aligned} \partial_\zeta B_n(\zeta) &= [-2in^2 - \sigma] B_n(\zeta) + \frac{1}{2}\sigma [B_{n+1}(\zeta) + B_{n-1}(\zeta)] \\ B_n(0) &= \delta_{n,0}. \end{aligned} \tag{26}$$

Now we make the central approximation

$$B_{n+1}(\zeta) + B_{n-1}(\zeta) - 2B_n(\zeta) \approx \frac{\partial^2}{\partial n^2} B_n(\zeta). \tag{27}$$

Therefore we must solve

$$\partial_\zeta B_n(\zeta) = -2in^2 B_n(\zeta) + \frac{1}{2}\sigma \partial_n^2 B_n(\zeta). \tag{28}$$

It can be confirmed by direct substitution that a solution condensing onto the $n = 0$ beam as $\zeta \rightarrow 0$ is

$$B_n(\zeta) \approx \frac{D}{\sqrt{\sinh(2\zeta\sqrt{i\sigma})}} \exp\left\{-n^2 \sqrt{\frac{i}{\sigma}} \coth(2\zeta\sqrt{i\sigma})\right\}. \tag{29}$$

But this solution is valid for large ζ , and cannot hold for $\zeta \rightarrow 0$. To see that it is indeed the correct solution of (28), and determine the constant D , we match to the small- ζ solution of (26) obtained by the analogue of the phase-grating procedure employed by Raman and Nath (1936a, 1936b) to solve their equations approximately, namely neglecting the term in n^2 . Then the solution of (26) is

$$B_n(\zeta) \approx \exp(-\sigma\zeta) I_n(\sigma\zeta) \tag{30}$$

where I_n is the modified Bessel function. This approximation satisfies the alternating sum rule (10) exactly. To match this to (29), we employ the Debye asymptotic approximations (Abramowitz and Stegun 1972) giving I_n for $\sigma\zeta$ and n large, and further approximate these for $\sigma\zeta \gg n$. Thus

$$\exp(-\sigma\zeta) I_n(\sigma\zeta) \approx \frac{\exp\left(-\frac{n^2}{2\sigma\zeta}\right)}{\sqrt{2\pi\sigma\zeta}}. \tag{31}$$

This matches precisely to (29) for small ζ , and enables D to be identified as

$$D = \frac{1}{\sqrt{\pi}} \left(\frac{i}{\sigma}\right)^{1/4}. \tag{32}$$

The final result is that the diffracted intensities are given by the Gaussian distribution

$$P_n = |A_n|^2 \approx a(\zeta, \sigma) \exp\left\{-\frac{n^2}{w(\zeta, \sigma)}\right\} \tag{33}$$

where the amplitude a and width w of the set of diffracted beams are

$$\begin{aligned} a(\zeta, \sigma) &= \frac{\sqrt{2}}{\pi\sqrt{\sigma}[\cosh(2\zeta\sqrt{2\sigma}) - \cos(2\zeta\sqrt{2\sigma})]} \\ w(\zeta, \sigma) &= \left(\frac{\sigma}{2}\right)^{1/4} \sqrt{\frac{\cosh(2\zeta\sqrt{2\sigma}) - \cos(2\zeta\sqrt{2\sigma})}{\sinh(2\zeta\sqrt{2\sigma}) + \sin(2\zeta\sqrt{2\sigma})}} \end{aligned} \tag{34}$$

This result should be valid for large σ .

If in addition $\zeta\sqrt{\sigma} \gg 1$, the amplitude decays exponentially and the width saturates:

$$\begin{aligned} a(\zeta, \sigma) &\rightarrow \frac{2}{\pi\sqrt{\sigma}} \exp\left(-\zeta\sqrt{2\sigma}\right) \\ w(\zeta, \sigma) &\rightarrow \left(\frac{\sigma}{2}\right)^{1/4} \end{aligned} \quad (\zeta\sqrt{\sigma} \gg 1). \tag{35}$$

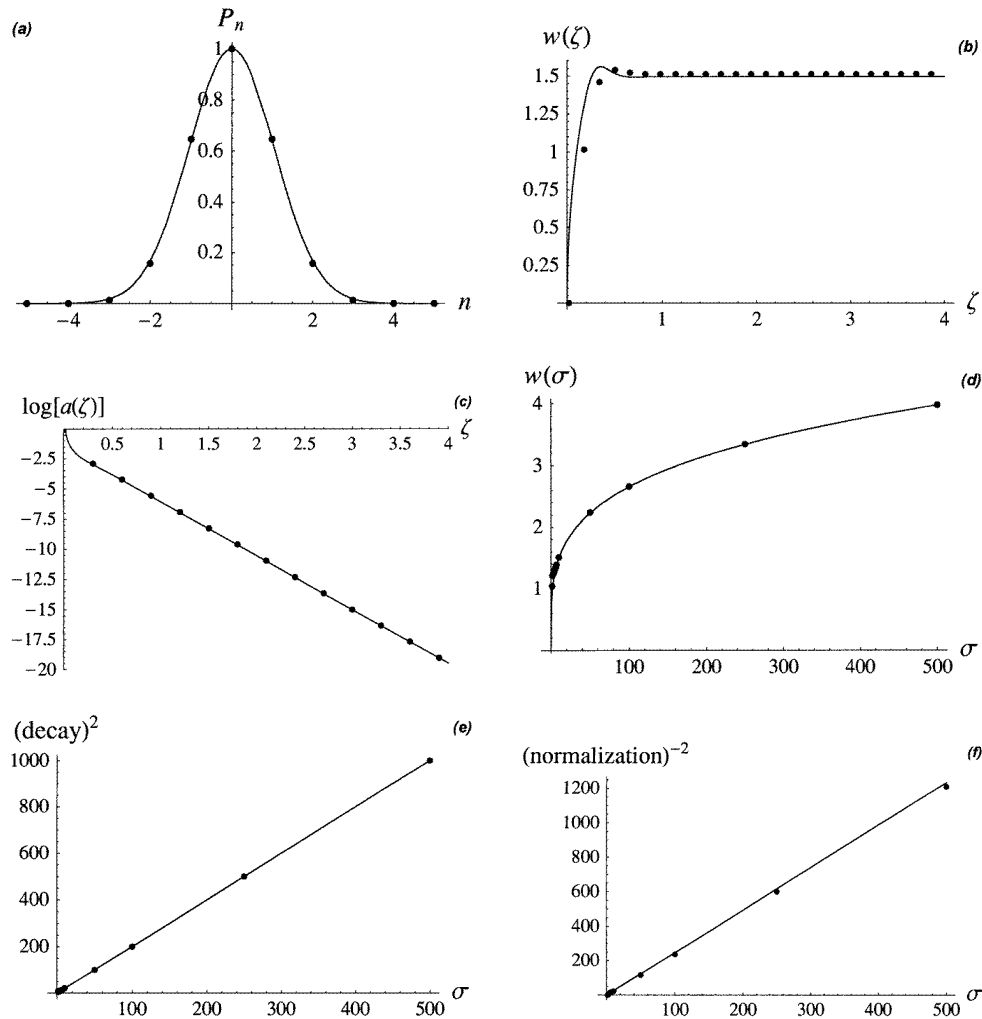


Figure 3. Dots: exact solutions of the Raman–Nath equations (8); full curves: calculations based on the semiclassical approximation (33) and (34). (a): Intensities for $\sigma = 10$, $\zeta = 4$. (b): Width w for $\sigma = 10$, fitted from exact solutions and calculated from (34). (c): As (b), but for the amplitude $\log a$. (d): Width w for large ζ , fitted from exact solutions and calculated from (35). (e): As (d), but for $(\text{decay constant})^2 = 2\sigma$ in amplitude a in (35). (f): As (e), but for $(\text{normalization})^{-2} = \sigma\pi^2/2$.

Comparison of the width with the corresponding result for transparent gratings ($n_{\max} \approx \sqrt{\sigma_2}$) shows that an imaginary grating of comparable strength transmits far fewer diffracted beams with appreciable intensity; in other words, the transmitted waves have a much narrower momentum distribution.

The arguments leading to (33) and (34) are not rigorous, and so it is desirable to test them against numerical solutions of the Raman–Nath equations (8). Figure 3 shows the comparisons. It is clear that the asymptotic intensities (33), with amplitude and width given by (34), gives an accurate description of diffraction by gratings with strong imaginary potentials, especially in the regime of large ζ that is so complicated for transparent gratings.

Acknowledgments

We thank A Zeilinger for drawing our attention to imaginary potentials in atom optics, and J H Hannay, W Schleich, and Y P Yakovlev for many informative discussions. D H J O'D was supported by a studentship from Bristol University. Partial support for this research was provided by a grant from the British Council, Austria.

References

- Abramowitz M and Stegun I A 1972 *Handbook of Mathematical Functions* (Washington: National Bureau of Standards)
- Berry M V 1966 *The Diffraction of Light by Ultrasound* (London: Academic)
- Berry M V 1994 Pancharatnam, virtuoso of the Poincaré sphere: an appreciation *Current Science* **67** 220–3
- Berry M V, Buxton B F and Ozorio de Almeida A M 1973 Between wave and particle—the semiclassical method for interpreting high-energy electron micrographs in crystals *Radiation effects* **20** 1–24
- Borrmann G 1941 Über Extinktionsdiagramme von Quarz *Phys. Z.* **42** 157–62
- Buxton B F and Berry M V 1974 *High-voltage Electron Microscopy* ed P Swann *et al* (London: Academic) pp 60–3
- Buxton B F and Berry M V 1976 Bloch wave degeneracies in systematic high energy electron diffraction *Phil. Trans. Roy. Soc. Lond. A* **282** 485–525
- Chudesnikov D O and Yakovlev V P 1991 Bragg scattering on complex potentials and formation of supernarrow momentum distributions of atoms in light fields *Laser Phys.* **1** 111–19
- Lucas R and Biquard P 1932 Propriétés optiques des milieux solides et liquides soumis aux vibrations élastiques ultra sonores *J. Phys. et Rad.* **3** 464–77
- Nomoto O 1951 Geometrical optical theory of the diffraction of light by ultrasonic waves. (1) Approximate treatment *Bull. Kobayasi Inst. Phys. Res.* **24** 42–71
- Oberthaler M K, Abfalterer R, Bernet S, Schmiedmayer J and Zeilinger A 1996 Atom waves in crystals of light *Phy. Rev. Lett.* **77** 4980–3
- Raman C V and Nath N S N 1936a The diffraction of light by high frequency sound waves: part I *Proc. Indian Acad. Sci. A* **2** 406–12
- Raman C V and Nath N S N 1936b The diffraction of light by high frequency sound waves: part IV, generalised theory *Proc. Indian Acad. Sci. A* **3** 119–25
- Teller E 1937 The crossing of potential surfaces *J. Phys. Chem* **41** 109–16